On the Performance Properties of the Minkowski Island Fractal Antennas

Ahmed M. Abdul-Lettif[1], M. A. Z. Habeeb[2], and H. S. Jaafar[3]

[1]College of Science, Babylon University

Hilla, Iraq, Email: abdullettif@yahoo.com

[2]Ministry of Science and Technology, Baghdad, Iraq

[3]College of Science, Karbala University, Karbala, Iraq

خواص الأداء لهوائيات منكوفسكي الكسورية

أحمد محمود عبد اللطيف،   محمد عبد الزهرة حبيب،   حيدر صادق جعفر

كلية العلو/ جامعة بابل،   وزارة العلوم والتكنلوجيا،   كلية العلوم/ جامعة كربلاء

الخلاصة

تمت دراسة خواص الاداء لهوائي الحلقة المربعة وهوائي مينكوفسكي ذي تكرار واحد وهوائي مينكوقسكي ذي تكرارين، وذلك باستعمال البرنامج الحاسوبي (NEC4).وقد اوضحت المحاكاة العددية ان هوائيات مينكوفسكي من الممكن ان تستعمل لتقليل حجم منظومات الهوائيات مع المحافظة على نفس الاداء الكهرومغناطيسي. وقد تبين ان هوائي مينكوفسكي ذا التكرار الواحد وهوائي مينكوفسكي ذا التكرارين لهما تصرف متعدد وعريض الحزم، وانه كلما ازداد عدد التكرار لهوائي منكوفسكي كلما ازداد التردد الرنيني وازداد عرض الحزمة. كما وجد انه بزيادة عدد التكرار للهوائي الكسوري فان كـلا من ربح الهوائي ومقاومة الدخول ونسبة فولتية الموجة الواقفة تقل، في حين ان انسجام الهوائي يتحسن.

Abstract

The performance properties of the square loop antenna (MO), Minkowski island of one iteration (M1), and Minkowski island of two iterations (M2) have been investigated using NEC4 which is moment-method- based software. The numerical simulations show that Minkowski island fractals can be used to achieve miniaturization in antenna systems while keeping an identical electromagnetic performance. It is demonstrated that M1 and M2 antennas exhibit multiband and broadband behavior, and as the number of iterations of the Minkowski fractal increases, the resonant frequencies increase and the bandwidth of each single band increases. Also, it is found that increasing the number of iterations of the fractal antenna causes a decrease in the antenna gain, input impedance, and voltage standing wave ratio, and it enhances the antenna matching

I. INTRODUCTION

With the widespread proliferation of telecommunication technology in recent years, the need for small-size multiband antennas has increased manifold. However, an arbitrary reduction in the antenna size would result in a large reactance and deterioration in the radiation efficiency. As a solution to minimizing the antenna size while keeping high radiation efficiency, fractal antennas can be implemented. A fractal is a rough or fragmented geometric shape that can be subdivided in parts, each of which is (at least approximately) a reduced-size copy of the whole [Mandelbrot(1983), Barnsley *et.al* (1988), Peitgen *et.al* (1990), and Jones *et.al* (1990)]. Fractal are space filling contours, meaning electrically large features can be efficiently packed into small areas [Falconer (1990) and Lauwerier (1990)]. Since the electrical lengths play such an important role in antenna design, this efficient packing can be used as a viable miniaturization technique. Miniaturization of a loop antenna using fractals was shown by Cohen [Cohen (1995) and Cohen (1996)]. A first attempt to explore the multifrequency properties of fractals as radiating structures was done by Puente and Pous [Puente and Pous (1996)].

In many cases, the use of fractal antennas can simplify circuit design, reduce construction costs, and improve reliability. Because fractal antennas are self-loading, no antenna tuning coils or capacitors are necessary. Often they do not require any matching components to achieve multiband or broadband performance. Fractal antennas can take on various shapes and forms. Among those currently reported in the literature include koch fractal [Puente *et.al* (1998)], the Sierpinski gasket [Puente *et.al* (1998) and Werner *et.al* (1998)], Hilbert curve [Vinoy *et.al* (2001)], and the Minkowski island fractals [Gianvittorio and Sami (2002)]. Some of these geometries have recently been pursued for antenna applications because of their inherent multiband nature. However, incorporation of fractal geometries into the antenna structures, and various aspects of their optimization, are still in the incipient stages. The majority of this paper will be focused upon the Minkowski island fractal antennas.

II. MINKOWSKI ISLAND FRACTAL GEOMETRY

In order for an antenna to work equally well at all frequencies, it must satisfy two criteria: it must be symmetrical about a point, and it must be self-similar, having the same basic appearance at every scale: that is, it has to be fractal. The shape of the fractal is formed by an iterative mathematical process. This process can be described by an iterative function system (IFS) algorithm, which is based upon a series of affine transformations [Werner and Ganguly (2003)]. An affine transformation in the plane ω can be written as:

$$\omega\begin{pmatrix} x_1 \\ x_2 \end{pmatrix} = Ax + t = \begin{pmatrix} r_1 \cos\theta_1 & -r_2 \sin\theta_2 \\ r_1 \sin\theta_1 & r_2 \cos\theta_2 \end{pmatrix} \begin{pmatrix} x_1 \\ x_2 \end{pmatrix} + \begin{pmatrix} t_1 \\ t_2 \end{pmatrix} \qquad (1)$$

where x_1 and x_2 are the coordinates of point x. If $r_1=r_2=r$ with $0<r<1$, and $\theta_1=\theta_2=\theta$, the IFS transformation is a contractive similarity (angles are preserved) where r is the

scale factor and θ is the rotation angle. The column matrix t is just a translation on the plane.

Applying several of these transformations in a recursive way, the Minkowski island fractals are obtained as depicted in Fig.1. The intiator is a square which can be regarded as a zeroth order of the Minkowski island fractal (MO). Each side of the square is modeled with 10 segments each of them has a length of 6 cm and a diameter of 2mm. The Minkowski island fractal of one iteration (M1) is formed by displacing the middle third of each side by some fraction of 1/3. By applying the same procedure on M1, the Minkowski island fractal of second iteration (M2) is obtained. It should be pointed out that the area of M1 is 37.4% smaller than that of MO, and the area of M2 is 54.5% smaller than that of MO.

III. NUMERICAL SIMULATIONS

Numerical simulations were done using NEC4 WIN95 VM, which is a moment-method-based software. The moment method implies an approximation of integral equations in terms of unknown currents $I(l)$ of the body [Stutzman and Thiele (1998) and Barlevy and Sami ((2001)]. The body may either be a length of perfectly conducting wire or a perfectly conducting surface. The integral equation for the unknown current $I(l)$ induced on the wires follows directly from enforcing the boundary condition, which implies that, the tangential component of the electric field vector to vanish on the surface of perfectly conducting wires. The moment method incorporates periodic boundary conditions. This allows for only one element of the periodic array to be simulated. When studying intricate elements such as fractals, this saves time and allows wide frequency sweeps that for some cases would not otherwise fit into the limitations of the computing hardware. Dielectrics were not incorporated, although some of the practical implementations do require dielectric support.

Since all details of the radiation pattern follow from knowledge of the electric and magnetic dipole moments of the charge and current distribution in the antenna, these factors should be analyzed. For MO antenna, the feed source is placed at the middle of the upper side. The current distribution resembled a sinusiod pattern. Through the program simulations, it was shown that the current is able to flow through the fractal wire almost as if it were flowing through a straight wire of the same effective length. The current distribution is given by

$$I_1 = -I_2 = \hat{y} \; I_0 \; \cos(ky) \qquad |y| \leq \frac{\lambda}{8} \qquad (2)$$

where I_1 and I_2 are the currents on the lower and upper sides of the square loop, and k is the wave vector.

$$I_4 = -I_3 = \hat{z} \; I_0 \; \sin(kz) \qquad |z| \leq \frac{\lambda}{8} \qquad (3)$$

where I_3 and I_4 are the currents on the left and right sides.

Since the vector potential (A) of the loop is in general given by [Stutzman and Thiele (1998)]

$$A = \mu \frac{e^{-jkr}}{4\pi r} \int_{loop} I e^{jk\hat{r}.r} dl \qquad (4)$$

and since the electric field vector (E) is given by

$$E_\theta = -jwA_\theta = -jwA.\hat{\theta} \qquad (5)$$

$$E_\phi = -jwA.\hat{\phi} \qquad (6)$$

then by using the expression [Stutzman and Thiele (1998)]

$$E_\theta = jw\mu \frac{2I_0}{k} \frac{e^{-jkr}}{4\pi r} \frac{\cos\left(\frac{\pi}{2}\cos\theta\right)}{\sin\theta} \qquad (7)$$

one can obtain

$$E_\theta = \left(\theta = \frac{\pi}{2}\right) = 0 \qquad (8)$$

$$E_\phi = \left(\theta = \frac{\pi}{2}\right) = \frac{jI_0\eta}{\sqrt{2}} \frac{e^{-jkr}}{2\pi r} \frac{\pi}{4}\left[\frac{\sin\left[\frac{\pi}{4}\cos\phi\right]}{\frac{\pi}{4}\cos\phi}\left[\sin\phi\cos\left(\frac{\pi}{4}\sin\phi\right) - \sin\left(\frac{\pi}{4}\sin\phi\right)\right] + \right.$$
$$\left. \frac{\cos\left[\frac{\pi}{4}\sin\phi\right]}{\frac{\pi}{4}\sin\phi}\left[\cos\phi\sin\left(\frac{\pi}{4}\cos\phi\right)\cos\left(\frac{\pi}{4}\cos\theta\right)\right] \right] \qquad (9)$$

Equation (9) gives the electric far field.

      Radiation patterns were generated at the resonant frequencies of the antenna. The resonant frequencies could be predicted from the plot of standing wave ratio (SWR) versus the frequency as shown in Fig.2. It can be noted from this figure that MO antenna has one resonant frequency at 135 MHz, M1 antenna has three resonant frequencies at 135, 248, and 480 MHz, and M2 antenna has four resonant frequencies at 135, 245, 335, and 455 MHz. It is interesting to note that Minkowski fractal antennas are not only broadband, but they also demonstrate multiband effects. This is due to the coupling between the wires. As more contours and iterations of the fractal are added, the coupling becomes more complicated and different segments of the wire resonate at different frequencies. It is worth mentioning that as the number of iterations of the fractal increases, the antenna has more resonant frequencies due to the self similarity in the geometry, and the bandwidth of each single band increases. The values of SWR for a 50 Ω transmission line at f=135 MHz for MO, M1, and M2 antennas are 2.62, 1.34, and 1.02 respectively. The radiation patterns at the resonant frequency of 135 MHz for MO, M1, and M2 antennas are shown in Fig.3. The corresponding three dimentional plots of the radiation patterns are depicted in Fig.4. It is interesting to note that the radiation patterns of MO, M1, and M2 antennas are

almost the same. This indicates that these antennas exhibit virtually identical electromagnetic radiation behavior, independent of the differences in antenna size and geometry. What is also worth mentioning is the similarity between the other band's patterns of each M1 amd M2 antenna. This is the proof for a truly multiband performance of the antenna.

The input impedance of a small linear diopole of length (l) and wire radias (a) can be approximated by [Balanis (1997)]

$$Z_{in} \cong 20\pi^2 \left(\frac{l}{\lambda}\right)^2 - j120 \frac{\left[\ln\left(\frac{l}{2a}\right) - 1\right]}{\tan\left(\pi\frac{l}{\lambda}\right)} \qquad (10)$$

Or it can be measured, as it is done in this work, by a rotation on the Smith chart to adjust the model of antenna to an RLC circuit. The Smith charts for MO, M1, and M2 antennas centered at the frequency of 135 MHz are depicted in Fig. 5. This figure shows that the matching of M2 antenna is better than the matching of M1 antenna, and this in turn is better than the matching of MO antenna. The input impedances of MO, M1, and M2 antennas at the frequency of 135 MHz are 124.83-j25.05Ω, 66.83-j2.14Ω, and 49-j0.5Ω respectively.

Other aspects of the Minkowski fractal antenna performance properties to consider are the gain and the half power beamwidth (HPBW). The gains of MO, M1, and M2 antennas relative to an isotropic source, which radiates equally in all directions, were computed to be 2.98, 2.62, and 2.32 dBi respectively. The HPBW was found to be 88° for MO antenna and 90° for each of M1 and M2 antenna. A summary of the performance properties of the investigated antennas at the resonant frequency of 135 MHz is presented in Table 1.

TABLE 1

PERFORMANCE CHARACTERISTICS OF THE MINKOWSKI ISLAND ANTENNAS AT THE RESONAT FREQUENCY

Parameter	MO Antenna	M1 Antenna	M2 Antenna
SWR	2.62	1.34	1.02
Input Impedance (Ω)	124.83-j25.05	66.83-j2.14	49-j0.5
Gain (dBi)	2.98	2.62	2.32
HPBW	88°	90°	90°
Reduction of Area	0%	37.4%	54.4%

IV. CONCLUSIONS

It is interesting to note that Minkowski fractal antennas are not only broadband, but they also demonstrate multiband effects. This is due to the coupling between the wires. As more contours and iterations of the fractal are added, the coupling becomes more complicated and different segments of the wire resonate at different frequencies. It is worth mentioning that as the number of iterations of the fractal increases, the antenna has more resonant frequencies due to the self similarity in the geometry, and the bandwidth of each single band increases. Minkowski island fractals can be used to achieve miniaturization in antenna systems while keeping an identical electromagnetic performance to the square loop antenna (M0). A size reduction of 37.4% was achieved using the M1 design over the M0 antenna. A further size reduction of 54.4% was achieved using the M2 design over the M0 antenna. It is interesting to note that the radiation patterns of MO, M1, and M2 antennas are almost the same. This indicates that these antennas exhibit virtually identical electromagnetic radiation behavior, independent of the differences in antenna size and geometry. What is also worth mentioning is the similarity between the other band's patterns of each M1 and M2 antenna. This is the proof for a truly multiband performance of the antenna.

REFERENCES

Balanis C. A. (1997) Antenna theory: analysis and design, 2nd Ed., New York, John Wiley & Sons.

Barlevy A. S. and Rahmat-Sami Y. (2001) "Charactrization of electromagnetic band-gaps composed of multiple periodic tripods with interconnecting vias concept, analysis and design", IEEE Trans. Antennas Propagat. vol. 49, no. 3.

Barnsley M. F., Devaney R. L., Mandelbrot B. B., Peitgen H. O., Saupe D., Voss R.F., Fisher Y., and Mc Guire M.(1988) The Science of Fractal Images, New York; Springer-Verlag.

Cohen N. (1995), "Fractal Antennas Part 1: Introduction and the Fractal Quad." Communications Quarterly Summer, pp: 7-22.

Cohen N. (1996), "Fractal Antennas Part 2: A Discussion of Relevant, but Disparate Qualities" Communications Quarterly Summer, pp: 53-66.

Falconer K.(1990), Fractal Geometry: Mathematical Foundations and Applications, New York, Johen Wiley & Sons.

Gianvittorio J. P. and Rahmat-Sami Y. (2002) " Fractal antennas: A noval miniaturization technique and applications", IEEE Antennas Propagat. Mag. vol. 44, no.1, pp. 20-36.

Jones H., Reeve D.E., and Saupe D.(1990), Fractals and Chaos, Crilly A. J., Earnshaw R. A., and Jones H., Eds. New York: Springer-Verlag.

Lauwerier H.(1991), Fractals: Endlessly Repeated Geometrical Figures, Princeton, New Jersey: Princeton University Press.

Mandelbrot B. B. (1983) The Fractal Geometry of Nature, San Francisco, CA: Freeman.

Peitgen H. O. , Jurgens H., and Saupe D.(1990) Chaos and Fractals, New York: Springer-Verlag..

Puente C. and Pous R. (1996)., "Fractal design of multiband and low side-lobe arrays", IEEE Trans. Antennas Propagat. Vol. 44, pp. 1-10.

Puente C., Romeu J. , Pous R., Ramis J., and Hijazo A. (1998) "Small but long Koch fractal monopole", Electron. Lett. vol. 34, pp. 9-10.

Puente C., Romeu J., Pous R., and Cardama A. (1998), "On the behavior of the Sierpinski multiband fractal antenna", IEEE Trans. Antennas Propagat. vol. 46, no. 4, pp. 517-524.

Stutzman W. I. and G. A. Thiele G. A. (1998) Antenna theory and design, John Wiley & Sons, New York.

Vinoy K. J., Jose K. A., Varadan V. K., and V. V. Varadan V. V.(2001) "Hilbert curve fractal antenna: A small resonant antenna for VHF/UHF applications, Microwave and Optical Technology Letters, vol. 29, no. 4, pp. 215-219.

Werner D. H. and Ganguly S. (2003) " An overview of fractal antenna engineering research", IEEE Antennas Propagat. Mag. vol. 45, no.1, pp. 36-56.

Werner D. H.,. Haupt R. L., and Werner P. L. (1999), "Fractal antenna engineering: the theory and design of fractal antenna arrays", IEEE Antennas Propagat. Mag. vol. 41, pp. 37-59.
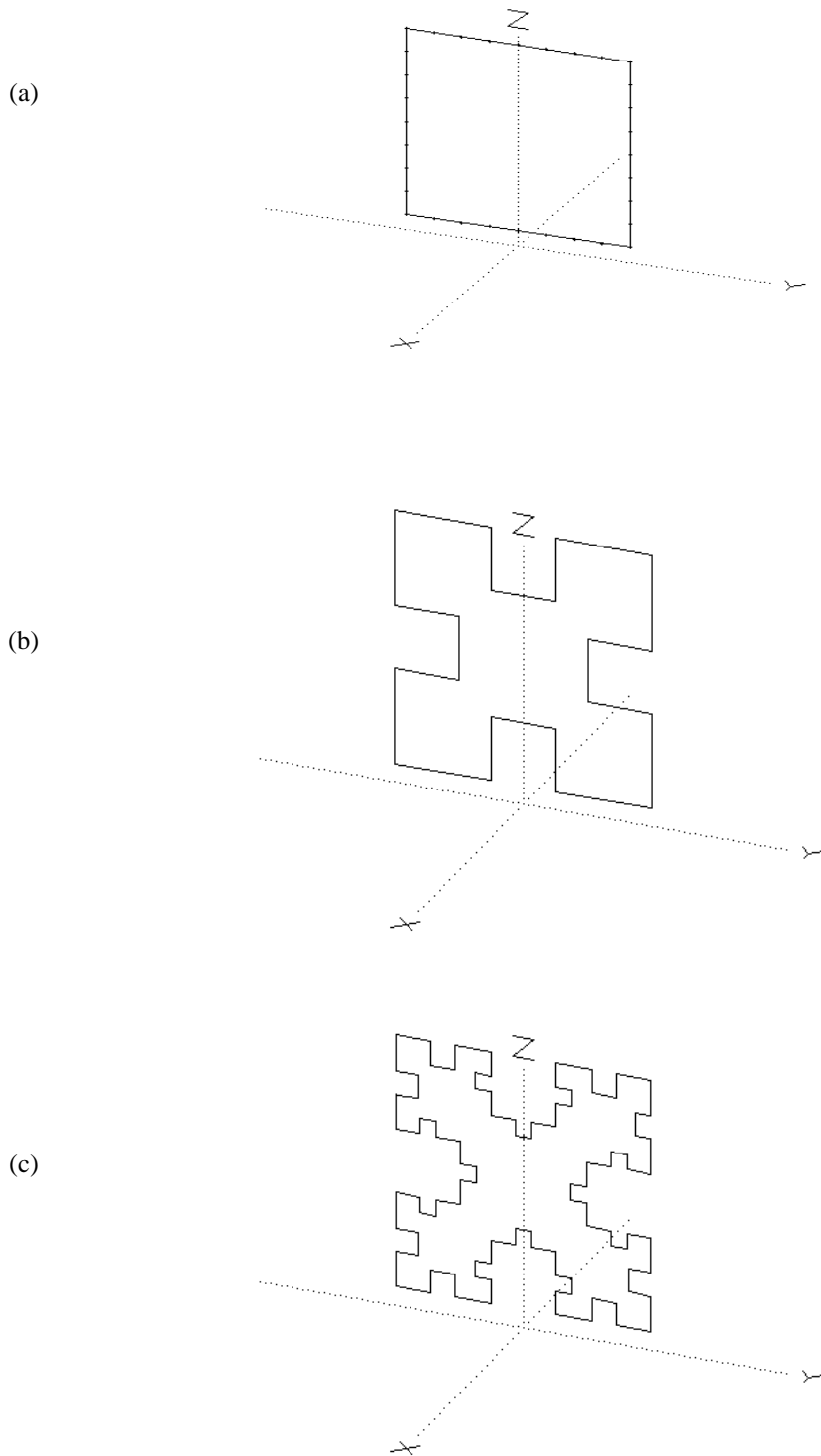
(a)

(b)

(c)

Fig. 1. Geometry of Minkowski island fractal of (a) zeroth order (MO), (b) one iteration (M1), and (c) two iterations (M2).
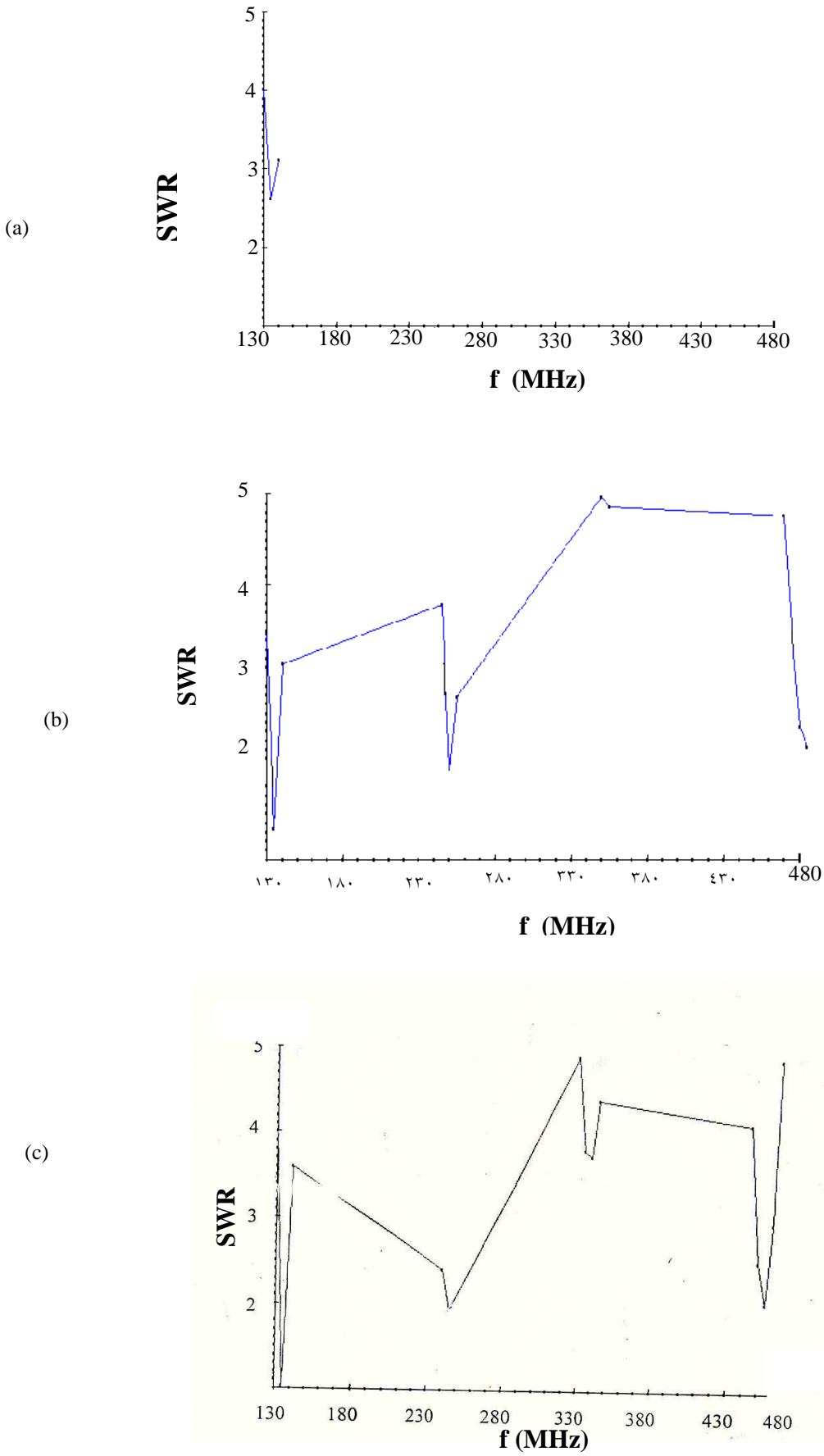
8

(a)

SWR

5

4

3

2

130   180   230   280   330   380   430   480

f (MHz)

(b)

SWR

5

4

3

2

۱۳۰   ۱۸۰   ۲۳۰   ۲۸۰   ۳۳۰   ۳۸۰   ٤۳۰   480

f (MHz)

(c)

SWR

5

4

3

2

130   180   230   280   330   380   430   480

f (MHz)

Fig. 2. SWR versus the frequency for (a) MO antenna, (b) M1 antenna, and (c) M2 antenna.

***Fig. 3. Radiation pattern at the resonant frequency of 135MHz for (a) MO
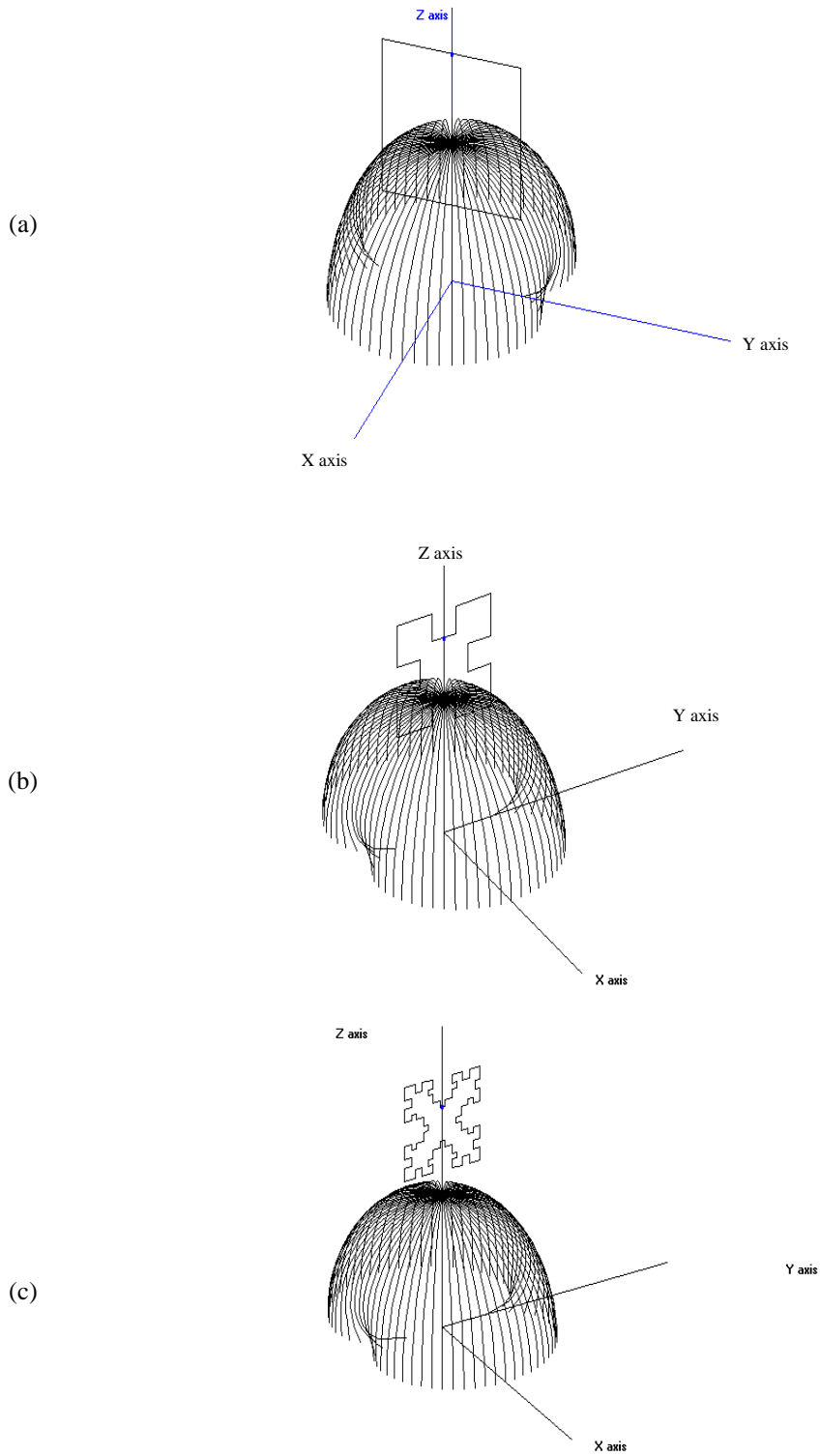antenna, (b) M1 antenna, and (c) M2 antenna.***

(a)

Z axis

Y axis

X axis

(b)

Z axis

Y axis

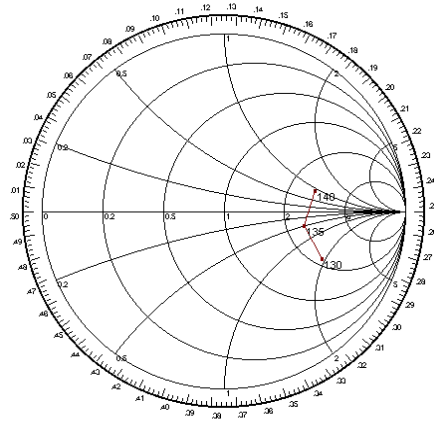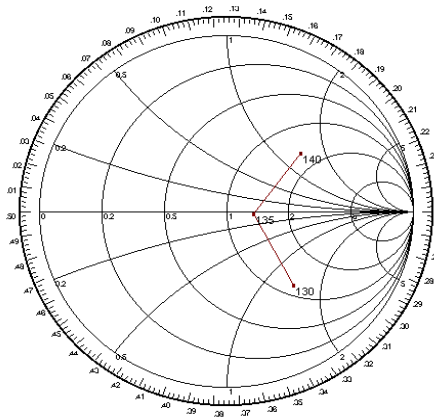X axis

(c)

Z axis

Y axis

X axis

Fig. 4. 3-D radiation pattern at the resonant frequency of 135MHz for (a) MO antenna, (b) M1 antenna, and (c) M2 antenna.
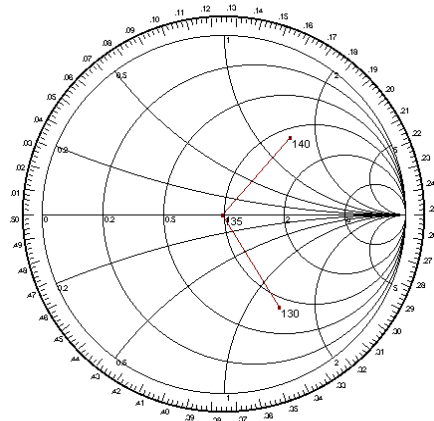
(a)

(b)

(c)

Fig. 5. Smith chart of (a) MO antenna, (b) M1 antenna, and (c) M2 antenna centered at 135MHz.